THE JOURNAL OF PHYSICAL CHEMISTRY B

Article

pubs.acs.org/JPCB

How Warfarin's Structural Diversity Influences Its Phospholipid Bilayer Membrane Permeation

Björn C. G. Karlsson,*[,†,⊥] Gustaf D. Olsson,[†,⊥] Ran Friedman,[‡,⊥] Annika M. Rosengren,[†,⊥] Henning Henschel,[†,¶,⊥] and Ian A. Nicholls[†,§,⊥]

[†]Bioorganic and Biophysical Chemistry Laboratory, Linnæus University Centre for Biomaterials Chemistry, Department of Chemistry and Biomedical Sciences, Linnæus University, SE-391 82 Kalmar, Sweden

[‡]Computational Chemistry and Biochemistry Group, Linnæus University Centre for Biomaterials Chemistry, Department of Chemistry and Biomedical Sciences, Linnæus University, SE-391 82 Kalmar, Sweden

[§]Department of Chemistry-BMC, Uppsala University, Box 576, SE-751 23 Uppsala, Sweden

[¶]Division of Atmospheric Sciences, Department of Physics, University of Helsinki, P.O. Box 64, Helsinki, Finland

Supporting Information

ABSTRACT: The role of the structural diversity of the widely used anticoagulant drug warfarin on its distribution in 1,2-dioleoyl-*sn*-glycero-3-phosphocholine (DOPC) bilayer membranes was investigated using a series of both restrained (umbrella sampling) and unrestrained molecular dynamics simulations. Data collected from unrestrained simulations revealed favorable positions for neutral isomers of warfarin, the open side chain form (OCO), and the cyclic hemiketal (CCO), along the bilayer normal close to the polar headgroup region and even in the relatively distant nonpolar lipid tails. The deprotonated open side chain form (DCO) was found to have lower affinity for the DOPC bilayer membrane relative to the neutral forms, with only a small fraction interacting with the membrane, typically within the polar headgroup region. The conformation of OCO inside the lipid bilayer was found to be stabilized by intramolecular hydrogen bonding thereby mimicking the structure of CCO. Differences in free energies, for positions of OCO and CCO inside the bilayer membrane, as compared to positions in the aqueous phase, were −97 and −146 kJ·mol^{-1}. Kinetic analysis based on the computed free energy barriers reveal that warfarin will diffuse through the membranes within hours, in agreement with experimental results on warfarin's accumulation in the plasma, thus suggesting a passive diffusion mechanism. We propose that this membrane transport may be an isomerization-driven process where warfarin adapts to the various local molecular environments encountered under its journey through the membrane. Collectively, these results improve our understanding of the influence of warfarin's structural diversity on the drug's distribution and bioavailability, which in turn may provide insights for developing new formulations of this important pharmaceutical to better address its narrow therapeutic window.

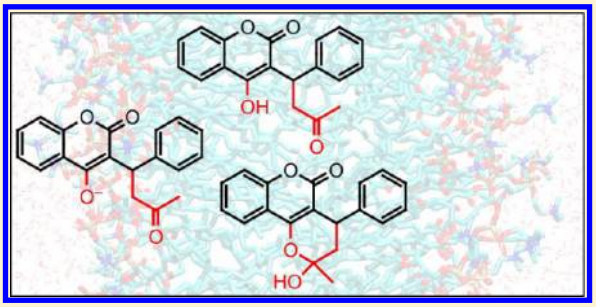

INTRODUCTION

The coumarin derivative warfarin, Chart 1, is a potent anticoagulant drug that inhibits the function of the active site of vitamin K dependent epoxide reductase (VKOR), and is commonly used for the prevention of thrombotic disorders such as myocardial infarction and stroke.[1,2] Despite being in widespread use and having a narrow therapeutic window, warfarin's mechanism of action is not yet completely understood. Importantly, difficulties in managing warfarin administration can result in severe side effects such as bleeding disorders and stroke.[3] A fact contributing significantly to the difficulties associated with the clinical use of warfarin is the coumarin's capacity to undergo a series of isomerization reactions,[4] where the preferred isomer is dictated by its environment, in particular, polarity and pH.[5−8] It has been shown that the cyclic hemiketal is the dominant form in the crystalline state,[9] though when binding to the blood plasma transport protein human serum albumin (HSA) it is present in the open side chain deprotonated state.[10] In addition to these observations, investigations of the modes of binding of warfarin to the liver enzyme cytochrome P450 2C9 have suggested that it is the cyclic hemiketal which binds to the active site of this enzyme.[11,12]

It is inferred that this demonstrated difference in the preferred structure for warfarin upon binding is strongly correlated to the nature of the binding site toward which the drug is directed.[13,14] Hence, detailed studies on the structural diversity of warfarin in various molecular microenvironments will provide insights on the mechanisms governing warfarin's distribution in vivo and potentially aid in predicting its

Received: January 9, 2013
Revised: February 1, 2013
Published: February 1, 2013

dx.doi.org/10.1021/jp400264x | *J. Phys. Chem. B* 2013, 117, 2384−2395

Chart 1. Phospholipid DOPC and Structural Forms of Warfarin Studied: Deprotonated DCO, Neutral Open Side Chain, OCO, and the Cyclic Hemiketal, CCO[a]

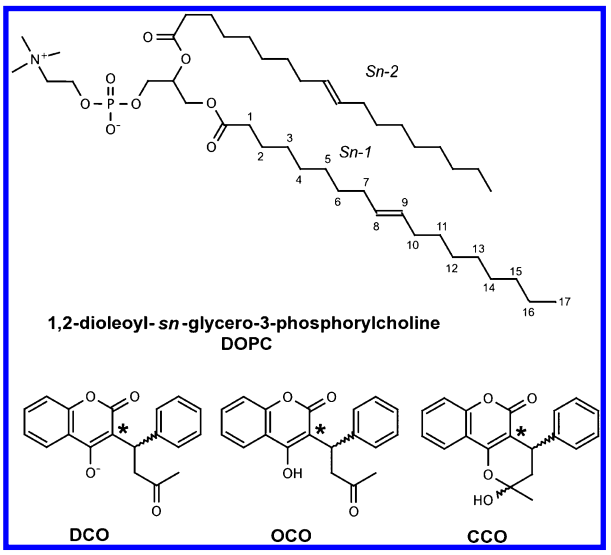

[a]The atom used as the approximate center of mass of warfarin, studied in unrestrained and umbrella sampling simulations, is marked with an asterisk.

biological effect.[15] Furthermore, since drugs have to undergo transport through membrane barriers in order to reach their targets, the study of the influence of isomeric form of warfarin on membrane permeation is highly motivated. The uptake of warfarin from the GI is essentially quantitative, and results in plasma concentrations that after 3−12 h correspond to the content of orally administrated doses;[16] however, the mechanisms of warfarin uptake through membrane barriers are still unknown. To shed further light on the origin of warfarin's structural diversity and possible influence of membrane permeation, Henschel et al.[17] recently reported a theoretical study on the mechanism of warfarin cyclic hemiketal formation. The authors suggested that warfarin isomerization is catalyzed through the involvement of water molecules, implying that hemiketal formation may occur at the water−lipid bilayer membrane interface where the polarity is different than that of bulk water. At this position, the electric dipoles of the phospholipid bilayer membrane and adjacent water molecules have significant impact on membrane structure, flexibility, and function.[18] To investigate the role of transmembrane carriers during hepatic uptake of warfarin, a recent in vivo study on the pharmacokinetics of warfarin involving 10 healthy volunteers by Frymoyer et al.[19] investigated the possibility of the involvement of a family of active membrane transporters, organic anion transporter polypeptides (OATPs).[20] This study was motivated by previous in vitro studies on rat and human hepatocytes showing strong inhibition of warfarin uptake in the presence of a nonspecific OATP inhibitor. Although the authors reported that OATP may not be clinically important in the in vivo pharmacokinetics of warfarin, the clear difference between the in vitro and the in vivo results led the authors to suggest further studies. Other studies on warfarin−membrane interactions have mostly involved artificial membrane systems. For example, experimental work by Avdeef et al.,[21] on liposomal membrane−water partitioning constants (log *P*) for warfarin using unilamellar vesicles of 1,2-dioleoyl-*sn*-glycero-3-phosphocholine (DOPC), Chart 1, demonstrated the problems with the octanol−water model for estimating membrane partitioning of ionizable drugs such as warfarin. The reported difficulties using this model in comparison with models based on lipid membranes could be attributed to the specific interaction formed between warfarin and the polar headgroup region of the lipid. The authors demonstrated, through the use of the pH metric technique,[22] that the largest difference in the experimentally determined log *P* was for the ionized form of warfarin which shifted from a log *P* of −0.46 to 1.38 when changing octanol to a liposomal system. The neutral form of warfarin was, however, only moderately affected by the change of model where its log *P* changed from 3.25 to 3.46. In another study, Huque et al.[23] examined the permeabilities for warfarin and 42 other ionizable drugs through membranes consisting of DOPC in dodecane. Results from these studies led to the conclusion that the presence of hydrogen bonding between the drug and the lipid bilayer strongly inhibited its permeation. On the same theme, Velický et al.[24] investigated the permeability of warfarin across artificial membranes (with DOPC lipids). Results from their studies revealed that warfarin exhibited high permeability that was strongly correlated to pH. The authors explained this correlation to be driven by an ion-pairing mechanism, in particular between the deprotonated form of warfarin and sodium ions, which facilitates the passive diffusion of charged warfarin species across the membrane. The importance of the formation of the sodium ion-pairing of the deprotonated open side chain form of warfarin for membrane permeation was also suggested by Cools and Janssen[25] after studying the effect on sodium ion concentration on permeation of warfarin across reverse-phase evaporation (REV) lipid vesicles of dipalmitoylphosphatidylcholine (DPPC) at pH 11.5. Although the authors in a previous paper[26] had reported the importance of sodium ion concentration for warfarin−membrane permeation, the later study involving DPPC REVs demonstrated no clear correlation. Together, these examples illustrate the complicated nature of the mechanisms involved when considering membrane permeation of warfarin.

Due to known experimental difficulties in obtaining detailed structural information on biomembranes in the liquid crystalline state,[27] previous studies of drug−membrane interactions have employed molecular dynamics (MD) simulations to characterize static equilibrium and kinetic properties of drugs in biomembranes.[28] Among a number of clinically and environmentally important substances that have been studied using the MD method are different psoralen derivatives,[29] pentachlorophenol,[30] valproic acid,[31] ubiquinone,[32] and recently also coumarin.[33] In all these studies, phospholipids have been of specific interest on account of them being a major component of cell membranes. To the best of our knowledge, studies investigating the role of warfarin's structural diversity on the nature of warfarin's transport over phospholipid bilayer membranes have not yet been reported.

In this study, we aim to shed light on the influence of warfarin's isomeric states on passive diffusion across phospholipid bilayer membranes. The three dominant structural forms of warfarin were studied in a fully solvated DOPC bilayer membrane. The major forms of the drug studied were the deprotonated, DCO, and neutral, OCO open side chain and the cyclic hemiketal, CCO, coumarins (Chart 1). The partitioning and the dynamics of warfarin transport in the model membrane were investigated using a series of unrestrained and restrained (umbrella sampling) molecular dynamics simulations. Parameters employed for the lipid

dx.doi.org/10.1021/jp400264x | J. Phys. Chem. B 2013, 117, 2384−2395

bilayer membrane used throughout this study were those previously presented by Rosso and Gould,[34] based on the recently developed general amber force field (GAFF).[35] The dynamics of the lipids were studied at 310 K, well above the gel to liquid crystalline phase transition temperatures, T_m, for DOPC (253 K).[36] While the interaction of warfarin with the membrane models has been experimentally examined in some previous studies, investigation of the influence of isomeric state on membrane partitioning, mobility, and distribution has not previously been undertaken. In this work, analysis of recorded MD simulation data revealed favorable positions of the neutral forms of warfarin, OCO and CCO, inside the nonpolar lipid tail region of DOPC. Interestingly, CCO was found to demonstrate a greater tendency to bind to the nonpolar lipid tails than OCO, which supports the previously observed preference of this structural form of the drug in nonpolar environments.[5−8] In all simulations, DCO was found to be largely distributed out in the aqueous phase or bound in the polar headgroup region of DOPC. This suggests that warfarin's permeation of phospholipid bilayer membranes may be explained by a process where changes in the local molecular environment provided by the DOPC bilayer membrane can induce changes in warfarin's isomeric distribution and thereby facilitating its permeation. In addition to this and considering its overall transport across phospholipid bilayer membrane an explanation involving active carriers cannot be neglected.

THEORETICAL CALCULATIONS

All simulations were conducted using the AMBER software package (v. 10.0, USCF, San Francisco, CA),[37] used with a combination of the AMBER (FF03)[38] and the general Amber (GAFF) force fields.[35] Initially, to obtain starting geometries for fully solvated phospholipid bilayer membrane systems incorporating various structural forms of warfarin, molecular models of pre-equilibrated bilayer membranes together with GAFF topology and parameter files for 1,2-dioleoyl-*sn*-glycero-3-phosphocholine (DOPC) were downloaded from the Richard Bryce group Web site at the University of Manchester, UK (http://www.pharmacy.manchester.ac.uk/bryce/amber#lip). This membrane model was published in 2008 by Rosso and Gould[34] and was one of the first cases reported where GAFF was successfully used for simulating a phospholipid bilayer membrane in the liquid-crystalline state without imposing any simulation bias such as constant area (NAT) or surface tension (NγT). The structural forms of warfarin investigated, OCO, DCO, and CCO (see Chart 1), were initially optimized using steepest descent (MMFF94) and a convergence criterion of 10^{-6} kcal·mol^{-1}. The geometries of these structures were then further optimized in Gaussian09,[39] using the default convergence criteria implemented in the software at HF/6-31G*, HF/6-31G**, and HF/6-31++G** levels of theory. GAFF parameters for the structural forms of warfarin used in this work as well as estimation of atomic partial charges, which were estimated through the restrained electrostatic potential (RESP) procedure, were obtained using the ANTECHAMBER module of the AMBER10 program. Force field parameters for the structural forms of warfarin can be found on pages S3−S7 in the Supporting Material. Since the estimated atomic partial charges of the different structural forms of warfarin studied did not change more than |0.13| of an electron charge, when going from the lowest to the highest levels of theory, the partial charges derived through the RESP-procedure on the structure optimized at the HF/6-31G* were used for further evaluation. It should be noted that GAFF was developed using partial charges determined using the HF/6-31G* basis set and it was therefore considered to be more reasonable to use the charges determined at this level of theory.

Unrestrained Simulations. Each warfarin−DOPC bilayer membrane model system simulated was built using PACKMOL.[40] Initially, explicit water molecules included in the downloaded pre-equilibrated bilayer membrane models were removed and the lipid bilayer membrane was placed in the middle of a virtual box with the same x and y dimensions as the lipid bilayer but elongated in the z dimension. The available space on either side of the lipid bilayer membrane was then packed with 1467 water molecules and one molecule of warfarin. Systems containing DCO were neutralized by the addition of sodium ions. The systems contained in total 72 phospholipid structures and 2934 water molecules (TIP3P[41]), and two copies of the same structural form of warfarin (and for some systems neutralizing sodium ions) were then subjected for a series of molecular dynamics (MD) steps using a similar equilibration procedure as previously described by Rosso and Gould.[34] In a first series of equilibration steps, each system was initially energy minimized to remove bad contacts created due to the packing procedure using a 500.0 kcal·mol^{-1}·Å^{-2} position restraint on the lipid bilayer, and thereafter allowing the whole system to relax without restraints. Here, a total number of 10 000 energy-minimization steps was undertaken whereof 5000 steps of steepest descent and 5000 steps of conjugate gradient. The temperature of the system was thereafter first raised from 0 to 310 K for 10 ps under constant volume and temperature (NVT) conditions, imposing a 10.0 kcal·mol^{-1}·Å^{-2} restraint on all lipids, before 300 ps of NPT simulation (1 bar, 310 K) was conducted using anisotropic pressure scaling and a pressure relaxation constant (τ_p) of 0.5 ps, while still applying a 10.0 kcal·mol^{-1}·Å^{-2} restraint on all the lipid molecules. Thereafter, the restraint on the lipid molecules was released in an additional 300 ps of simulation. The τ_p was at this point increased to 1.0 ps for 500 ps and then to its final value of 2.0 ps for the rest of the total simulation time of 61.61 ns for the warfarin−DOPC systems. During MD simulations, the temperature was held constant using Langevin dynamics with a collision frequency (gamma_ln) of 1.0 ps^{-1}. Throughout all simulations bonds to hydrogen atoms were constrained using the SHAKE algorithm, allowing a time step of 0.002 ps. During equilibration and collection of production phase data, periodic boundary conditions were applied in all directions using a 10 Å nonbonded interaction cutoff. Here, long-range electrostatics were treated using the particle mesh Ewald summation method, and long-range van der Waal interactions were corrected using a continuum model correction of both energy and pressure. To improve the statistics in the collection of warfarin−phospholipid bilayer membrane data, each system simulated was built in triplicate after randomly packing the warfarin structures studied in the water phase of each system while holding the equilibrated coordinates of the lipid bilayer membranes unchanged. As reference, a fully solvated DOPC membrane without warfarin was simulated using the same procedure as being described above. Note that MD equilibration data are available for the first series of simulations, extracting data from the last 10 ns of the 50−60 ns region for each unrestrained DOPC membrane system in both the absence and presence of structural forms of warfarin (Table S1 in the Supporting Information). In addition to this first round of unrestrained simulations, an additional 100 ns of unre-

dx.doi.org/10.1021/jp400264x | J. Phys. Chem. B 2013, 117, 2384−2395

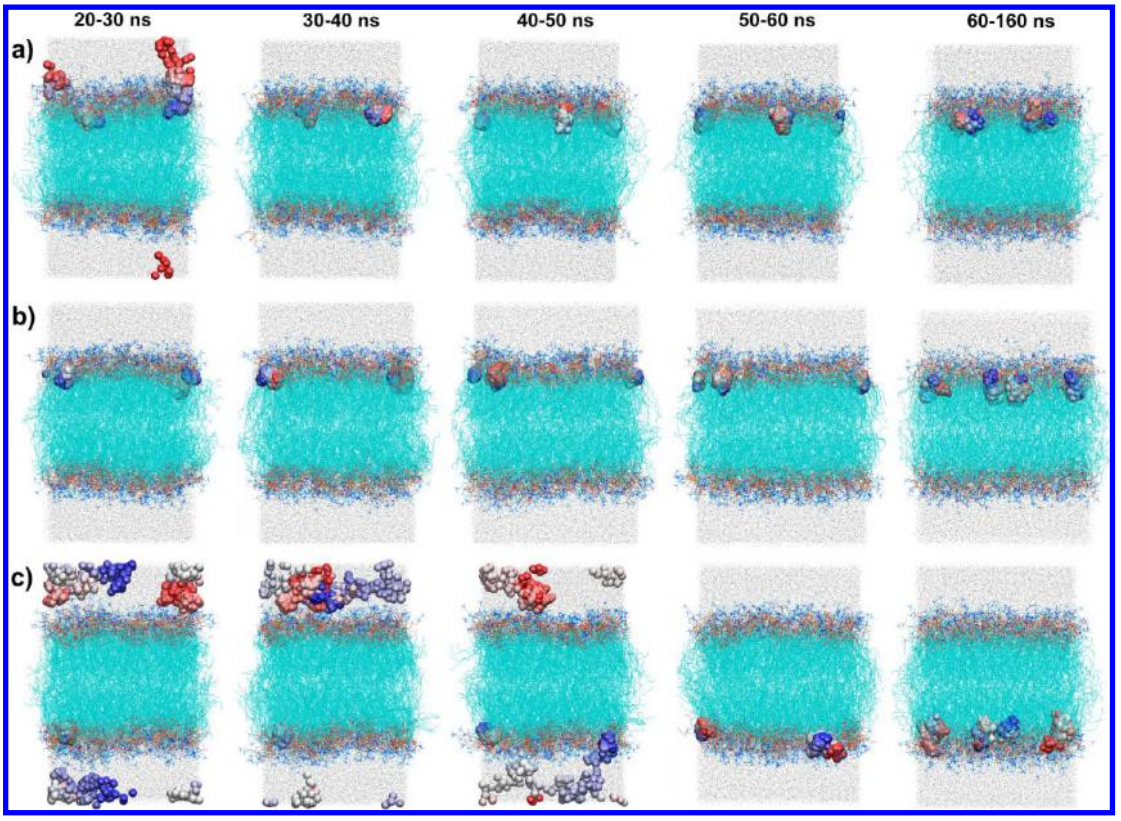

Figure 1. Overlaid snapshots from independent simulations (a, b, and c), each containing two molecules of OCO in a DOPC bilayer membrane (DOPC and water oxygen (in gray) as line representations) demonstrating the dynamics during 20−160 ns as the mobility of the center of mass of OCO (see Chart 1, here as van der Waal's volume representation, using time-step coloring, where red color indicates snapshots from the beginning of each presented simulation interval, white color representing intermediate snapshots, and blue color snapshots from the end of each presented simulation interval). Every frame presented is the sum of a total of 500 snapshots for OCO (extracted every 0.02 ns for 10 ns simulation windows and every 0.2 ns for dynamics between 60 and 160 ns) and 10 snapshots for water oxygens and DOPC lipids (extracted every 1 ns for 10 ns simulation windows and every 10 ns for dynamics between 60 and 160 ns), respectively.

strained simulation was collected and analyzed. Finally, to investigate the dynamics of warfarin inside the lipid tail part of DOPC, unrestrained simulations of 50 ns were performed, using starting coordinates for a single molecule of either OCO or CCO, which initially was inserted and equilibrated in the bilayer center from a series of umbrella sampling simulations. See below for a description on how the umbrella sampling simulations were performed.

Umbrella Sampling (US). The DOPC bilayer−warfarin coordinates, obtained after 61.61 ns of simulation, were used as the starting coordinates for a series of umbrella sampling (US) simulations. These simulations were performed identically as described above, although using a different series of equilibration steps and routines for sampling different restrained positions along the DOPC bilayer normal (*z*-axis) for the structural forms of warfarin studied. In these sets of calculations, one of the two structures of warfarin previously inserted was removed and two dummy atoms were inserted (with nonbonded interaction turned off), one in the center of the bilayer membrane and the other one at a 35 Å distance from the first dummy atom along the bilayer normal. The positions of these inserted dummy atoms were restrained using a force constant of 100 kcal·mol^{-1}·Å^{-2} throughout all steps of the US calculations. The systems were subjected to a series of new equilibration steps. First, energy minimization (500 steps of steepest descent and 500 steps of conjugate gradient) was performed followed by 50 ps of equilibration at NVT and 200 ps of equilibration at NPT prior to a longer equilibration step (200 ps) at NPT, where the distance of the center of mass (COM) of the structures of warfarin studied (Chart 1) was initially restrained at 0.01 Å from the dummy atom inserted in the center of the bilayer using a distance restraint of 2 kcal·mol^{-1}·Å^{-2}. Moreover, to keep the dummy atom at its position in the bilayer membrane, the distance between the COM of all phosphate atoms of the DOPC polar head groups and the single dummy atom placed in the bilayer center, was position restrained throughout the simulations using a distance restraint of 100 kcal·mol^{-1}·Å^{-2}. Second, in a further equilibration step, an additional restraining potential was introduced where the angle between the COM of warfarin and the two dummy atoms was restrained to 180° using an angle restraint of 30 kcal·mol^{-1}·rad^{-2}. This final equilibration step was run for 200 ps prior to collecting production phase data for 500 ps, both at condition of NPT. After sampling data at 0.01 Å from the center of the DOPC bilayer membrane, an additional 30 biased US windows were collected from sampling of the distances every 1 Å up to 30 Å from the dummy atom placed in the bilayer center. In all steps of the US calculations, an equilibration step of 200 ps was performed prior to collecting data during 500 ps at each restrained distance. Altogether, a total number of 31 biased US windows were investigated totally sampling 15.5 ns of data along the bilayer membrane normal for each structural form of warfarin studied. The sampled histogram data (see Figure S8 in the Supporting

dx.doi.org/10.1021/jp400264x | *J. Phys. Chem. B* 2013, 117, 2384−2395

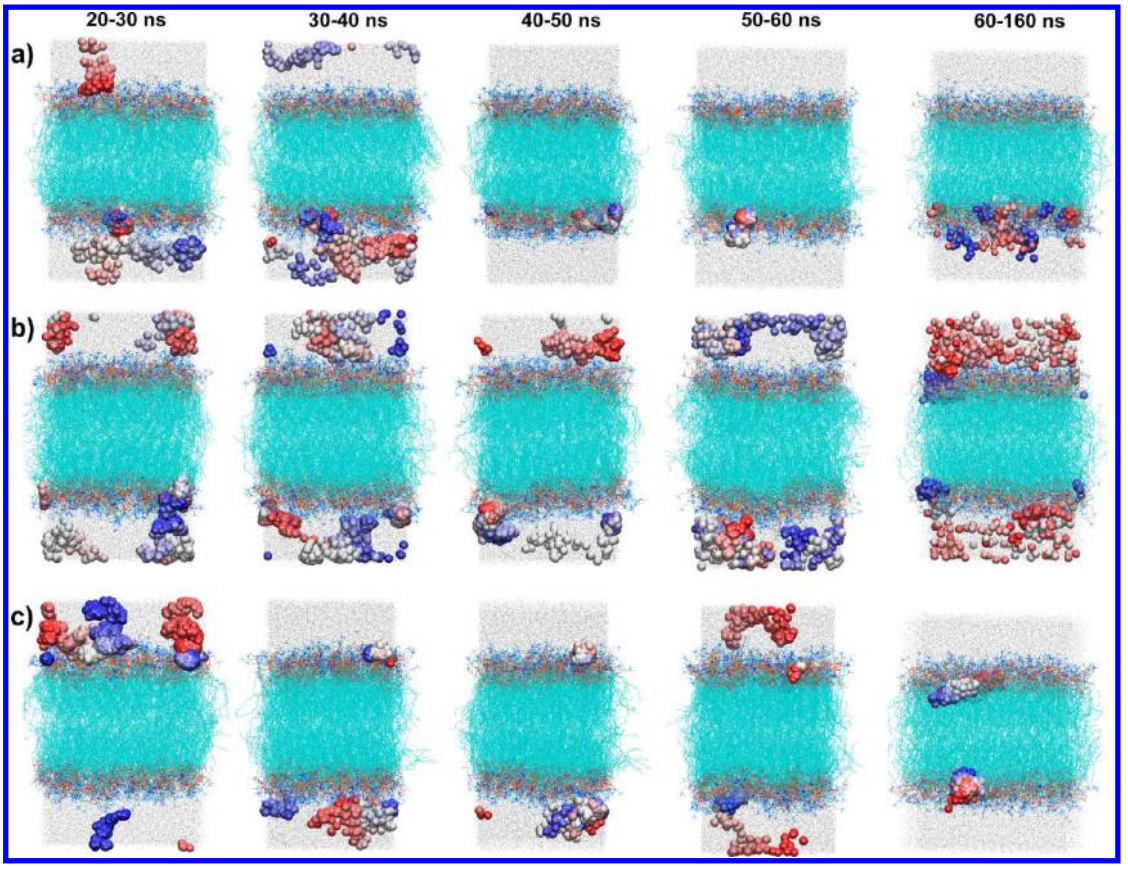

Figure 2. Overlaid snapshots from independent simulations (a, b, and c), each containing two molecules of DCO in a DOPC bilayer membrane (DOPC and water oxygen (in gray) as line representations) demonstrating the dynamics during 20−160 ns as the mobility of the center of mass of DCO (see Chart 1, here as van der Waal's volume representation, using time-step coloring, where red color indicates snapshots from the beginning of each presented simulation interval, white color representing intermediate snapshots, and blue color snapshots from the end of each presented simulation interval). Every frame presented is the sum of a total of 500 snapshots for DCO (extracted every 0.02 ns for 10 ns simulation windows and every 0.2 ns for dynamics between 60 and 160 ns) and 10 snapshots for water oxygens and DOPC lipids (extracted every 1 ns for 10 ns simulation windows and every 10 ns for dynamics between 60 and 160 ns), respectively.

Information) were thereafter analyzed using the weighted histogram analysis method (WHAM)[42] to obtain relative free energies for positions along the DOPC bilayer normal through the calculation of potentials of mean force (PMFs).

RESULTS AND DISCUSSION

Initially, a series of calculations was performed using a set of commonly used descriptors for characterizing the relative success of computer simulations of biomembranes such as lipid surface area, volume per lipid and deuterium order parameters (S_{CD}) (see Figures S4−S5 and Table S2 in the Supporting Information). The simulated behavior of the DOPC lipid bilayer membrane was in full agreement with previously published data by Rosso and Gould,[34] demonstrating a phospholipid bilayer membrane in the liquid crystalline state. Recent studies highlighting the structural diversity of warfarin, in particular its influence on bioavailability,[7,15,17] motivate deeper investigation of the structure−function relationship of this coumarin derivative. Initially, to determine the mobility, partitioning and possible preferred location of each of the structural forms of warfarin present in the fully hydrated DOPC membrane studied, each simulated bilayer membrane system was analyzed after recording 160 ns (rejecting the first 1.61 ns of equilibration data) of unrestrained trajectory data. Subsequent extraction of trajectory data, where the position and the dynamics of the center of mass (COM, see Chart 1) for all structural forms of warfarin was tracked during simulations, suggested that the transition from the water to the lipid phase of the neutral forms of warfarin (the open side chain, OCO, and the cyclic hemiketal, CCO) is a barrierless process and occurs on a time scale covered by the simulation, within 50−60 ns for OCO (Figure 1) and 30−40 ns for CCO (Figure 3). Inside the bilayer, kinetically accessible regions for OCO and CCO were positions along the bilayer normal close to the polar headgroup−nonpolar lipid tail region of DOPC. These parts of the lipid bilayer have previously been described as regions 2 and 3 of the four-region model first presented by Marrink and Berendsen and are regions with high density of polar head groups and lipid acyl chains.[43] It was also recently shown by Paloncýová and co-workers that this part of the DOPC bilayer membrane is populated by coumarin through a barrierless transition process into the DOPC bilayer which occurrs within a 10 ns time frame.[33] Estimations of the distance for the COM of OCO and CCO from the bilayer center, during 50−60 ns of simulation, revealed kinetically accessible bilayer normal positions approximately 11−17 Å from the bilayer center, Figures S6 and S7 in the Supporting Information. Interestingly, inspection of the final positions of warfarin inside the bilayer after additionally 100 ns of simulation revealed no further diffusion into the lipid tail parts of the DOPC bilayer. It may be suggested that the faster diffusion of CCO into the membrane compared to OCO, as was already observed during the first

dx.doi.org/10.1021/jp400264x | J. Phys. Chem. B 2013, 117, 2384−2395

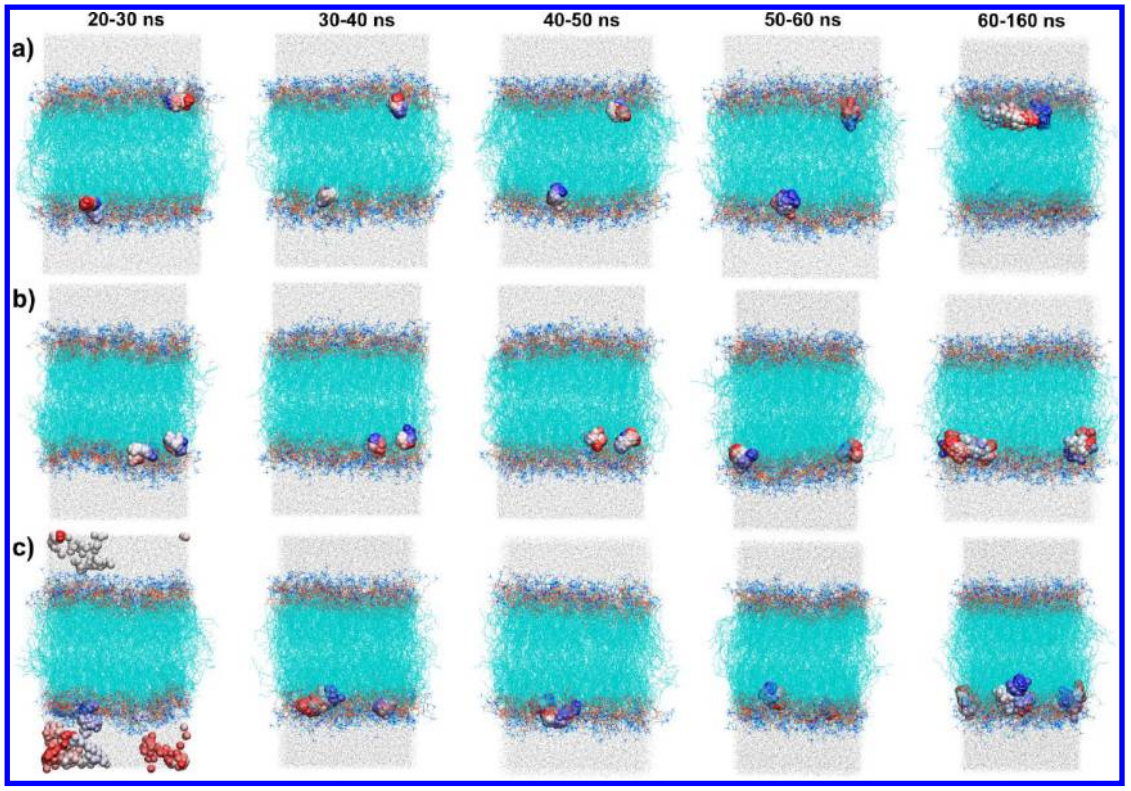

Figure 3. Overlaid snapshots from independent simulations (a, b, and c), each containing two molecules of CCO in a DOPC bilayer membrane (DOPC and water oxygen (in gray) as line representations) demonstrating the dynamics during 20−160 ns as the mobility of the center of mass of CCO (see Chart 1, here as van der Waal's volume representation, using time-step coloring, where red color indicates snapshots from the beginning of each presented simulation interval, white color representing intermediate snapshots, and blue color snapshots from the end of each presented simulation interval). Every frame presented is the sum of a total of 500 snapshots for CCO (extracted every 0.02 ns for 10 ns simulation windows and every 0.2 ns for dynamics between 60 and 160 ns) and 10 snapshots for water oxygens and DOPC lipids (extracted every 1 ns for 10 ns simulation windows and every 10 ns for dynamics between 60 and 160 ns), respectively.

50−60 ns of simulation, may be explained by a difference in affinity for the bilayer membrane.

To shed further light on the time scale needed to reach convergence in membrane positions of warfarin, OCO and CCO were inserted into the bilayer membrane center. Thereafter, 50 ns of simulation data, a time scale similar to the transition from water into the lipid phase, were collected and analyzed. Analysis of the dynamics of OCO and CCO in this series of simulations revealed, however, a diversity in final bilayer normal positions where some of the molecules investigated had a position in agreement with positions found after 160 ns of simulation, using starting coordinates in the aqueous phase, whereas other molecules were found to be located inside the lipid tail region of DOPC (Figure S11 in the Supporting Information). These results indicate the long time scales needed to sample diffusion processes, and even that the global energy minima for these structural forms may not be represented by bilayer normal positions found after a transition from water to the lipid membrane phase occurring within more than 160 ns of simulation.

In contrast to the positions found for OCO and CCO inside the DOPC lipid bilayer, the deprotonated open side chain form of warfarin, DCO, which is responsible for binding to HSA as well as inhibiting VKOR function, was demonstrating much lower affinity for the membrane. Compared to the neutral isomers, the weaker binding of DCO to the bilayer membrane was reflected by the preferential position of DCO covered by the polar headgroup by DOPC (Figure 2). In contrast to membrane-bound OCO and CCO, some molecules of DCO were observed to bind and then become released from the polar headgroup region out in the aqueous phase. During the last part of the simulation, between 60 and 160 ns, however, a small fraction of the molecules of DCO studied was found to be able to penetrate the polar headgroup region of DOPC and to also be distributed into the nonpolar lipid tail part of DOPC. Altogether, the observed diffusion behavior of DCO is typical for an ionic species and indicates the necessity for alternative or complementary mechanisms in order to permit membrane transport, e.g., active transport or a role for warfarin's isomerization.

Additionally, during a total of 1.92 μs (12 × 160 ns) of unrestrained simulation starting initially in the aqueous phase, none of the 12 molecules of either OCO or CCO were found to permeate across the DOPC bilayer membrane or even diffuse from one bilayer leaflet to another. To be able to overcome energy barriers along the bilayer normal and thereby obtain quantitative descriptions on the probabilities and free energies for passive diffusion of OCO and CCO across the DOPC bilayer membrane studied, a series of umbrella sampling (US) simulations was conducted. Collected distance histograms from these simulations (Figure S8 in the Supporting Information) were analyzed using the WHAM method to generate the potential of mean force (PMF).[44] Calculated free energy profiles, PMFs, for OCO and CCO provided further support for the favorable localization of these isomers around the polar headgroup and lipid tail region of DOPC. For OCO

dx.doi.org/10.1021/jp400264x | J. Phys. Chem. B 2013, 117, 2384−2395

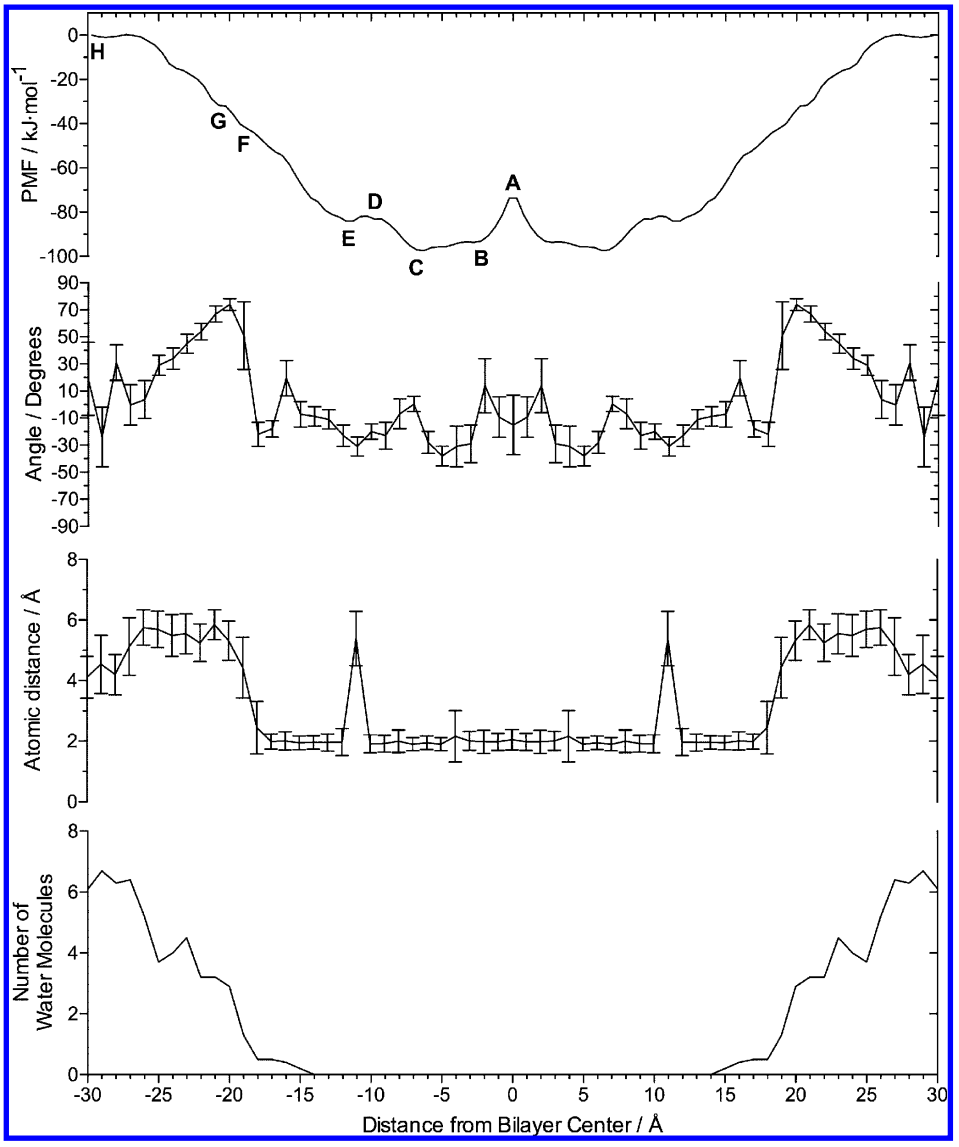

Figure 4. Results from umbrella sampling of OCO for varying restrained center-of-mass positions along the DOPC bilayer normal: the potential of mean force (PMF), the corresponding variation in the vector describing the angle of the coumarin ring with respect to the bilayer normal (z-axis), the atomic distance of the carbonyl oxygen atom of the side chain and the hydroxyl hydrogen of the phenol-type hydroxyl group of OCO, and finally, the average number of water molecules found around OCO. Although the umbrella sampling was performed along a z-coordinate representing half the bilayer, for symmetry reasons results obtained for that part has been duplicated to give a full representation of the whole bilayer. Bold inserted letters A–H in the PMF represent snapshots from umbrella sampling and which are presented in Figure 5.

(Figures 4 and 5), a local minimum in the PMF was found at ∼12 Å, a position along the bilayer normal populated already during the initial 50–60 ns of unrestrained simulation, but also a global minimum found at ∼7 Å from the bilayer center. Interestingly, the corresponding PMF for CCO (Figures 6 and 7) demonstrated a global minimum, at a bilayer membrane normal position similar to that found for OCO, ∼8 Å from the bilayer center. Moreover, as was observed from unrestrained simulations, where diffusion into the polar headgroup region of DOPC occurred within 50–60 ns when starting in the aqueous phase, the computed PMF suggested that the warfarin water–lipid transition is a barrierless process, in total agreement with the previously observed transitions for coumarin and its derivatives 7-acetoxy- and 7-acetoxy-4-methylcoumarin into lipid membranes.[33] Computed relative free energies for positions of OCO and CCO at the global minima yielded approximately −97 and −146 kJ·mol^{-1} for positions in the membrane in comparison with a position far out into the aqueous phase, 30 Å from the bilayer center for OCO and CCO, respectively. Additionally, the free energy barrier for transversion from one leaflet to another (over the bilayer center) was approximately 9 kT for OCO and 11 kT for CCO. These computed values suggest that the permeation of OCO and CCO within the lipid tails of DOPC from one leaflet to another is probable (with an estimated energy barrier limit of approximately 16 kT).[33] Kinetic analysis, based on the theory of activation energy, previously used for coumarin,[33] yielded an estimation of the time scale for membrane permeation of warfarin occurring within hours for OCO (approximately 1 h for 50% transport of OCO). In addition, the strong interaction of CCO with the membrane resulted in a corresponding value for its transport that is significantly longer than its half-time ($t_{1/2}$ = 42 h).

dx.doi.org/10.1021/jp400264x | J. Phys. Chem. B 2013, 117, 2384–2395

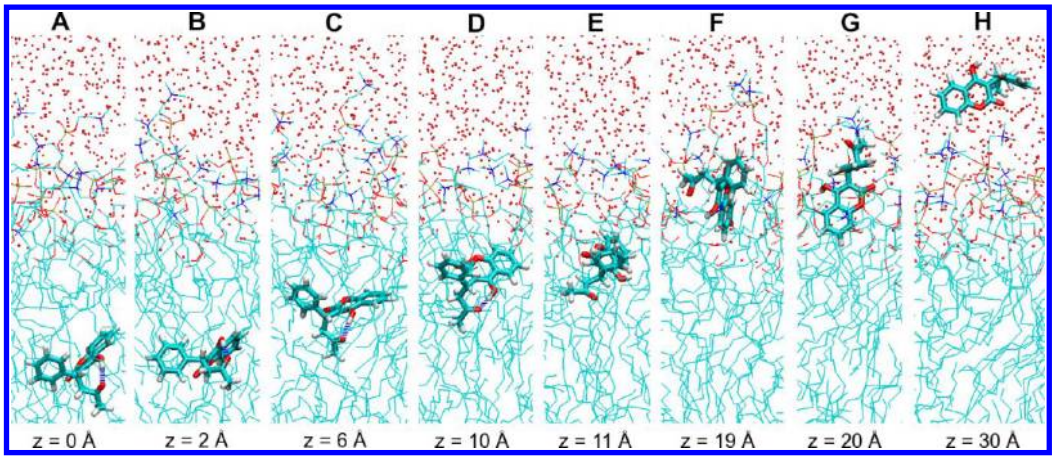

Figure 5. Selected snapshots from the umbrella sampling simulation of OCO along different restrained distances in the DOPC bilayer membrane. The letters above each frame represent regions in the calculated PMF as presented in Figure 4. Here, warfarin is shown as a licorice representation with a blue dashed line between functionalities involved in intramolecular hydrogen bonding, and DOPC and the water oxygen atoms are shown as line representations.

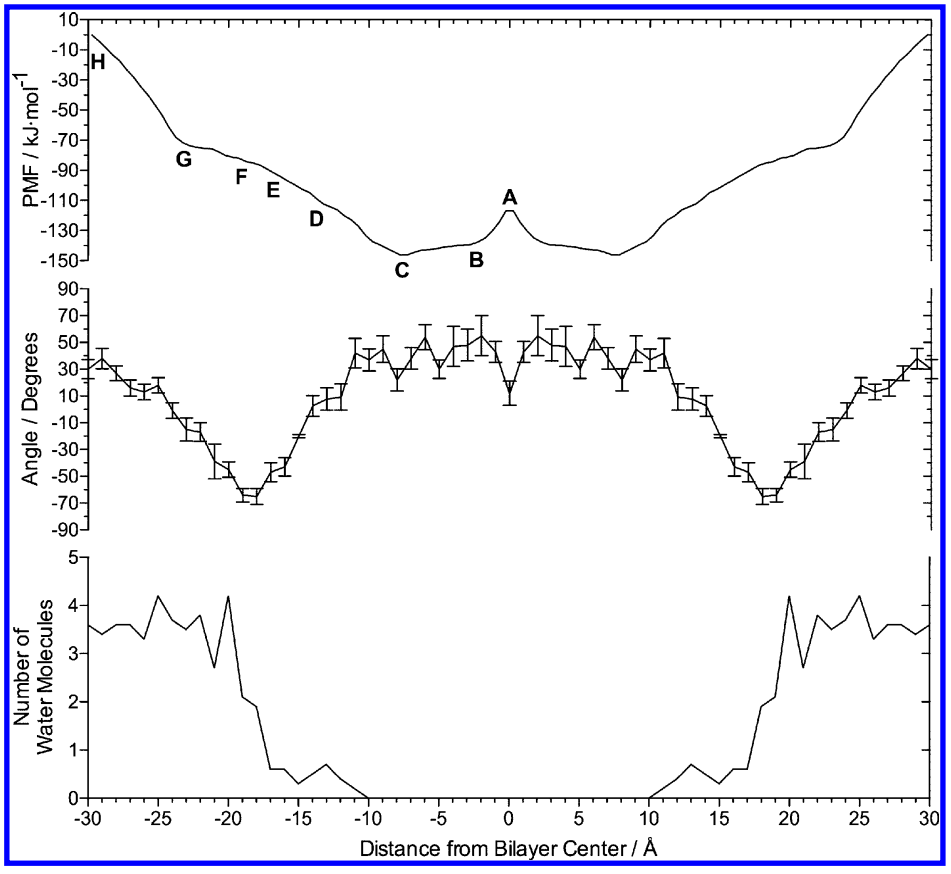

Figure 6. Results from umbrella sampling (US) of CCO for varying center-of-mass positions along the DOPC bilayer normal: the potential of mean force (PMF), the corresponding variation in the vector describing the angle of the coumarin ring with respect to the bilayer normal (z-axis), and the average number of water molecules found around CCO. Although the US was performed along a z-coordinate representing half the bilayer, results obtained for that part has been duplicated to give a full representation of the whole bilayer. Bold inserted letters A–H in the PMF represent snapshots from US presented in Figure 7.

To further describe orientations and conformations of the neutral forms of warfarin positioned along the bilayer normal during US simulations, the angle of the coumarin ring of warfarin with respect to the bilayer normal as well as the average number of water molecules solvating warfarin at the various positions along the bilayer normal were calculated. Furthermore, due to the capability of OCO to form an intramolecular hydrogen bond, the atomic distance of the hydrogen atom of the phenolic hydroxyl group and the carbonyl oxygen of the side chain were calculated at each bilayer position. Interestingly, a study of variation in the coumarin backbone–bilayer normal angle throughout the US simulations revealed that, for both OCO and CCO, the coumarin moiety was found in the plane of the bilayer in the

dx.doi.org/10.1021/jp400264x | J. Phys. Chem. B 2013, 117, 2384–2395

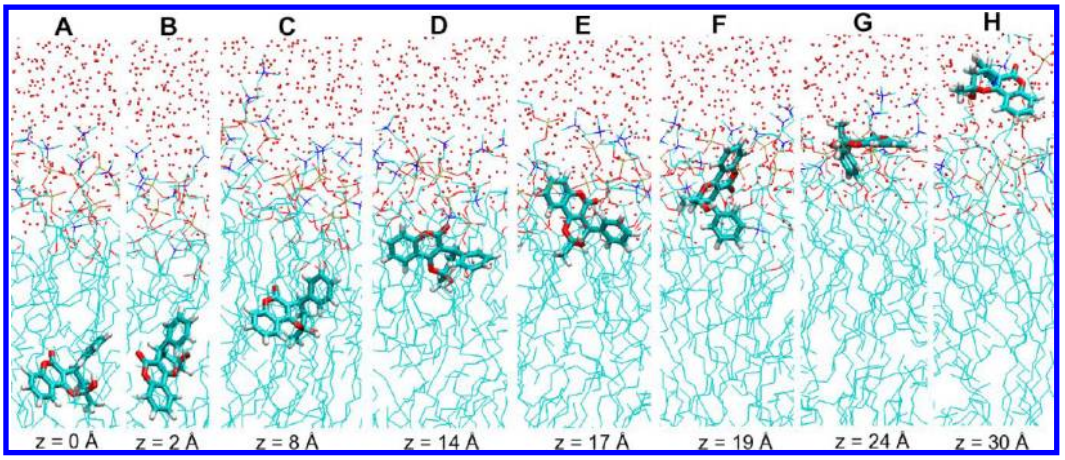

Figure 7. Selected snapshots from umbrella sampling of CCO along different restrained distances in the DOPC bilayer membrane. The letters above each presented frame represent interesting regions in the calculated potential of mean force as presented in Figure 6. In this figure, warfarin is shown as a licorice representation, and the DOPC lipid and the water oxygen atoms are shown as a line representations.

nonpolar lipid tail part of DOPC, whereas when located in the polar headgroup region (starting approximately at 18−19 Å from the bilayer center), the orientation was found to be roughly parallel to the bilayer plane. This favorable orientation of the coumarin backbone can be observed in Figures 4 and 6 as well as in selected snapshots from US, especially 19 Å and 20 Å for OCO (snapshots F and G in Figure 5) and 17 and 19 Å for CCO (snapshots E and F in Figure 7). The roughly parallel orientation of the coumarin backbone with respect to the bilayer normal was also recently suggested by Paloncýová et al.,[33] who reported on an orientation of the coumarin ring with the oxygen turned upward toward the aqueous phase when positioned inside the membrane.

Furthermore, a possible explanation for the rotation of the warfarin molecule when located at a position close to the polar headgroup region, as observed in the simulations and in the selected snapshots, is that it is caused by the preferential positioning of the more hydrophobic parts of the warfarin molecule, notably the phenyl group in the lipid portion of the membrane. This behavior was especially evident in simulations of CCO where the hydrophobic phenyl group was retained in the lipid region as the distance from the bilayer center was increased. A more detailed analysis of the behavior of OCO in the lipid tail part of the membrane clearly indicated that OCO formed an intramolecular hydrogen bond in these regions of the membrane; see snapshots A−E in Figure 5 for examples. This behavior is in agreement with previous simulations of this form of the drug in pure organic solvents, such as chloroform.[6] Furthermore, it may be assumed that the formation of this intramolecular hydrogen bond in OCO affords a structure mimicking that of the hemiketal isomer, CCO, which has been shown by a range of NMR[8] and UV[5] spectroscopic techniques to be the most stable form of warfarin under nonpolar conditions.

An interesting observation can be made upon inspecting the sudden breaking of the intramolecular hydrogen bond of OCO at approximately 10−12 Å from the bilayer center. At this position, the presence of double bonds in the lipid tails clearly seem to provide a steric hindrance for the intramolecular conformation of OCO. Another important observation is that the two minima found in the calculated PMF for OCO (B−E in the PMF in Figure 4 or selected snapshots in Figure 5) are located around this position in the membrane, thus indicating localization of this structural form of warfarin in the vicinity of the double bonds of DOPC. Based upon this observation, it may be concluded that CCO is also located at this bilayer normal position, 7−8 Å from the bilayer center, corresponding to the global minima found in PMFs. Analysis of the distance between side-chain groups of OCO during unrestrained simulation, initially starting out in the aqueous phase, demonstrated the absence of intramolecular hydrogen bonding at bilayer normal positions found during 160 ns of simulation. It did, however, reveal distances between side-chain groups similar to the distances found for DCO (Figures S12 and S13 in the Supporting Information).

The importance of intramolecular hydrogen bonding in OCO was demonstrated after initially inserting OCO in the bilayer center and thereafter extracting simulation data during 50 ns. Here, OCO was found to be intramolecularly hydrogen bonded to positions along the bilayer normal, ∼10−12 Å from the bilayer center, approximately at the local minimum found for OCO in the calculated PMF. Interestingly, an analysis of the dynamics of the COM of OCO and CCO revealed trans-versions from one leaflet to another (Figure S14 (OCO) and Figure S18 (CCO) in the Supporting Information) in accordance with the relatively low energy barrier computed in the PMF. Furthermore, analyses of variations of the angle of the coumarin backbone with respect to the bilayer plane during unrestrained simulation gave further support to that reported from PMF calculations, revealing typically only a restricted number of allowed conformations of warfarin inside the high density regions of the DOPC bilayer membrane, as compared to regions of lower density 0−5 Å from the bilayer center (Figures S15−S18).

Finally, to investigate the importance of water solvation inside the lipid bilayer membrane, the average number of water molecules was calculated after integration of the generated radial distribution functions (RDFs) describing the probability of finding the oxygen atom of water within a 5 Å distance from the COM atom of warfarin. Results for neutral forms of warfarin show that the bilayer normal position, 0−10 Å from the bilayer center, is free from water. It should be noted that due to the relatively low free energy barriers associated with diffusion inside the lipid tail region of DOPC, warfarin is, when located close to the polar headgroup region, partially solvated by water molecules. It is therefore reasonable to assume that

dx.doi.org/10.1021/jp400264x | J. Phys. Chem. B 2013, 117, 2384−2395

this change in local molecular microenvironment can drive the conversion of one isomer into another as discussed by Henschel and co-workers.[17] Furthermore, it is highly probable that this mechanism is governing the permeation of warfarin, especially if there is a difference in pH between the regions separated by the membrane.

US simulations of DCO, at various positions along the DOPC bilayer membrane were performed using starting coordinates from unrestrained simulations after 61.61 ns, resulted in the inclusion of a solvation shell of water molecules around this form of the drug even in the nonpolar membrane core. This tendency of water molecules to associate with the negative charge of DCO was also observed in simulations which were started after having initially removed the water molecules that followed warfarin during equilibration in the bilayer center (this additional series of simulations is entitled DCO* in the Supporting Information, Figures S9 and S10). This unusual behavior has previously been reported in simulations of the amino acid arginine,[45,46] in attempts to model the effect of the charged amino acid residue, or its side-chain analogue *n*-propylguanidinium,[47] upon exposure to nonpolar regions in membrane-bound proteins. Problems with the parametrization of membranes have been proposed to be a general problem for the simulation of charged species in pure nonpolar domains.[48] Although the GAFF parameters used for the DOPC lipid studied are clearly not optimal for describing contacts with charged molecular species, the response of this model membrane to the inclusion of DCO in the nonpolar lipid core of the DOPC bilayer membrane clearly reflects the energetically unfavorable environment provided by the lipid tails. In addition to this observation, results obtained from the series of unrestrained simulations of DCO suggested that the nonpolar membrane lipid core provides a barrier to warfarin's permeation in conjunction with results obtained by us from previous experimental and theoretical investigations using a combination of UV spectroscopy and DFT-based predictions, demonstrating the absence of DCO in nonpolar solvents such as chloroform and *n*-heptane.[5] Based upon these observations, it may be suggested that the passive diffusion of DCO across the DOPC bilayer membrane is unlikely and hence other mechanisms must be involved when this structural form of the drug is transported across membranes, e.g., an isomerization-dependent process.

As has been previously stated in this paper, this process is not static (which is an assumption made by the classical MD treatment of the warfarin isomers and DOPC lipids) and more elaborate treatments may be needed to fully investigate the role of warfarin's structural diversity on its permeation through phospholipid bilayer membranes.

CONCLUSIONS

In this paper, we have investigated the diffusion properties of three major structural forms of the oral anticoagulant drug warfarin in a fully solvated DOPC bilayer membrane, as a model for phospholipid bilayer membranes. The DOPC membrane model chosen is compatible with the general Amber force field (GAFF) developed to be especially suitable for small organic drug molecules such as warfarin for simulations with biomacromolecules such as proteins and DNA. The role of warfarin's structural diversity on passive diffusion through a series of fully solvated DOPC bilayer membranes was initially investigated using 3 μs of unrestrained simulation for warfarin in a DOPC bilayer membrane revealing favorable bilayer normal positions of the neutral isomers, the open side chain form (OCO) and the cyclic hemiketal (CCO), inside the nonpolar lipid tail region. The deprotonated open side chain form, DCO, was found to have lower affinity for the fully solvated DOPC bilayer membrane studied. In addition, no sodium ion−DCO complexation was observed during simulations, as has previously been reported in studies on warfarin binding to artificial membranes (see Figure S19 in the Supporting Information). Umbrella sampling revealed detailed information regarding free energies, preferred orientations, and degree of intramolecular hydrogen bonding as well as the degree of aqueous solvation at the various positions investigated along the DOPC bilayer membrane normal. Relative free energies for the positions in the bilayer membrane compared with the aqueous phase were approximately −97 and −146 kJ·mol^{-1} for OCO and CCO, respectively. Corresponding calculations for DCO resulted in an anomalous aqueous solvation of this form of warfarin even in the lipid nonpolar tail core of the membrane, indicating that GAFF-based parameters used inadequately describe such interaction. Detailed studies on the orientation of the neutral forms of warfarin in the DOPC bilayer membrane suggested that penetration of the polar headgroup region of DOPC leads to an orientation of the coumarin ring backbone of warfarin which is roughly parallel to the normal of the bilayer membrane. Well inside the lipid tail core of the membrane, the angle of the coumarin ring was, however, found to adopt a more perpendicular orientation to the bilayer plane. Interestingly, OCO was found to be strongly intramolecularly hydrogen bonded inside the nonpolar core of the membrane, thereby mimicking the molecular structure of CCO. This mimicry is reflecting the stability of CCO under nonpolar conditions. The results presented herein highlight the importance of warfarin's isomerism when considering permeation of this important oral anticoagulant drug across phospholipid bilayer membranes. The high free energy barriers calculated for both neutral forms of warfarin as well as the low affinity observed for DCO leads to the conclusions that the transport of warfarin across phospholipid bilayer membranes is regulated via a mechanism which is governed by a molecular environment change in the isomeric distribution of warfarin. Interestingly, experimental evidence from O'Reilly et al. shows that the concentrations of warfarin in patients plasma reach peak levels after 3−12 h.[16] Kinetic analysis of the energy barriers for the transportation of warfarin into the membranes[33] reveals that the mean time of transportation of warfarin over the membrane by passive diffusion for OCO is on the order of hours (approximately 1 h for 50% transport of OCO). The strong interaction of CCO with the membrane resulted in a corresponding value for its transport that is orders of magnitude longer than the lifetime of the molecule in the body ($t_{1/2}$ = 42 h). Thus, our analysis suggests that warfarin undergoes passive diffusion, although we cannot rule out other mechanisms. Moreover, the insights gained may improve possibilities for avoiding problems arising from warfarin's narrow therapeutic window and even for the development of controlled release formulations for this important pharmaceutical.

ASSOCIATED CONTENT

Supporting Information

General Amber force field (GAFF) parameters for structural forms of warfarin (OCO, DCO, and CCO), molecular dynamics equilibration data, lipid surface area data, volume

dx.doi.org/10.1021/jp400264x | J. Phys. Chem. B 2013, 117, 2384−2395

per lipid data, deuterium order parameter data, polar headgroup z-axis distribution over time (region between 50 and 60 ns), represented by choline nitrogen or phosphorus atom of the phosphate group or the center-of-mass atomic distribution of OCO, DCO, or CCO in the DOPC bilayer membranes, potentials of mean force for DCO, selected snapshots from umbrella sampling of DCO, and histograms of from the biased umbrella sampling simulations of OCO, DCO, DCO*, and CCO. Snapshots from unrestrained (50 ns) simulations of OCO and CCO, initially inserted in the bilayer center. Variations in bilayer normal positions (OCO, DCO, and CCO), distance between side groups (OCO and DCO), and coumarin backbone−bilayer plane angles (OCO, DCO, and CCO) during unrestrained simulations, starting either out in the aqueous phase (60−160 ns) or in the center of the bilayer (50 ns). Frequency histograms for variation in sodium ion−DCO distances, starting out in the aqueous phase (20−160 ns). This material is available free of charge via the Internet at http://pubs.acs.org.

AUTHOR INFORMATION

Corresponding Author

*E-mail: bjorn.karlsson@lnu.se.

Author Contributions

$^{\perp}$The manuscript was written with contributions from all authors. All authors have given approval to the final version of the manuscript.

Notes

The authors declare no competing financial interest.

ACKNOWLEDGMENTS

The simulations were performed on resources provided by the Swedish National Infrastructure for Computing (SNIC) at Lunarc (Platon). The financial support from the Swedish Research Council (VR), the Knowledge Foundation (KKS), Crafoord Foundation, Carl-Tryggers' Foundation, and the Linnæus University is most gratefully acknowledged.

REFERENCES

(1) Li, T.; Chang, C.-Y.; Jin, D.-Y.; Lin, P.-J.; Khvorova, A.; Stafford, D. W. *Nature* **2004**, *427*, 541−544.

(2) Rost, S.; Fregin, A.; Ivaskevicius, V.; Conzelmann, E.; Hortnagel, K.; Pelz, H. J.; Lappegard, K.; Seifried, E.; Scharrer, I.; Tuddenham, E. G. D.; et al. *Nature* **2004**, *427*, 537−541.

(3) Landefeld, C.; Beyth, R. *Am. J. Med.* **1993**, *95*, 315−328.

(4) Porter, W. R. *J. Comput. Aided Mol. Des.* **2010**, *24*, 553−573.

(5) Karlsson, B. C. G.; Rosengren, A. M.; Andersson, P. O.; Nicholls, I. A. *J. Phys. Chem. B* **2007**, *111*, 10520−10528.

(6) Karlsson, B. C. G.; Rosengren, A. M.; Andersson, P. O.; Nicholls, I. A. *J. Phys. Chem. B* **2009**, *113*, 7945−7949.

(7) Rosengren, A. M.; Karlsson, B. C. G. *Biochem. Biophys. Res. Commun.* **2011**, *407*, 318−320.

(8) Valente, E. J.; Lingafelter, E. C.; Porter, W. R.; Trager, W. F. *J. Med. Chem.* **1977**, *20*, 1489−1493.

(9) Valente, E. J.; Trager, W. F.; Jensen, L. H. *Acta Crystallogr.* **1975**, *B 31*, 954−960.

(10) Petitpas, I.; Bhattacharya, A. A.; Twine, S.; East, M.; Curry, S. *J. Biol. Chem.* **2001**, *276*, 22804−22809.

(11) Heimark, L. D.; Trager, W. F. *J. Med. Chem.* **1984**, *27*, 1092−1095.

(12) He, M.; Korzekwa, K. R.; Jones, J. P.; Rettie, A. E.; Trager, W. F. *Arch. Biochem. Biophys.* **1999**, *372*, 16−28.

(13) Karlsson, B. C. G.; Rosengren, A. M.; Näslund, I.; Andersson, P. O.; Nicholls, I. A. *J. Med. Chem.* **2010**, *53*, 7932−7937.

(14) Nicholls, I. A.; Karlsson, B. C. G.; Rosengren, A. M.; Henschel, H. *J. Mol. Recognit.* **2010**, *23*, 604−608.

(15) Rosengren, A. M.; Karlsson, B. C. G.; Nicholls, I. A. *ACS Med. Chem. Lett.* **2012**, *3*, 650−652.

(16) O'Reilly, R. A.; Aggeler, P. M.; Leong, L. S. *J. Clin. Invest.* **1963**, *42*, 1542−1551.

(17) Henschel, H.; Karlsson, B. C. G.; Rosengren, A. M.; Nicholls, I. A. *J. Mol. Struct. (Theochem)* **2010**, *958*, 7−9.

(18) Gawrisch, K.; Ruston, D.; Zimmerberg, J.; Parsegian, V. A.; Rand, R. P.; Fuller, N. *Biophys. J.* **1992**, *61*, 1213−1223.

(19) Hagenbuch, B.; Meier, P. *Biochim. Biophys. Acta (BBA), Biomembr.* **2003**, *1609*, 1−18.

(20) Frymoyer, A.; Shugarts, S.; Browne, M.; Wu, A. H. B.; Frassetto, L.; Benet, L. Z. *Clin. Pharmacol. Ther.* **2010**, *88*, 540−547.

(21) Avdeef, A.; Box, K. J.; Comer, J. E. A.; Hibbert, C.; Tam, K. Y. *Pharm. Res.* **1998**, *15*, 209−215.

(22) Avdeef, A.; Box, K. .; Comer, J. E. .; Gilges, M.; Hadley, M.; Hibbert, C.; Patterson, W.; Tam, K. . *J. Pharm. Biomed. Sci.* **1999**, *20*, 631−641.

(23) Huque, F. T. T.; Box, K.; Platts, J. A.; Comer, J. *Eur. J. Pharm. Sci.* **2004**, *23*, 223−232.

(24) Velický, M.; Bradley, D. F.; Tam, K. Y.; Dryfe, R. A. W. *Pharm. Res.* **2010**, *27*, 1644−1658.

(25) Cools, A.; Janssen, L. *Int. J. Pharm.* **1984**, *20*, 335−346.

(26) Cools, A. A.; Janssen, L. H. M. *J. Pharm. Pharmacol.* **1983**, *35*, 689−691.

(27) Nagle, J. F.; Tristram-Nagle, S. *BBA, Rev. Biomembr.* **2000**, *1469*, 159−195.

(28) Tieleman, D. P. *Clin. Exp. Pharmacol. Physiol.* **2006**, *33*, 893−903.

(29) Dos Santos, D. J. V. A.; Eriksson, L. A. *Biophys. J.* **2006**, *91*, 2464−2474.

(30) Mukhopadhyay, P.; Vogel, H. J.; Tieleman, D. P. *Biophys. J.* **2004**, *86*, 337−345.

(31) Ulander, J.; Haymet, A. D. J. *Biophys. J.* **2003**, *85*, 3475−3484.

(32) Soderhall, J. A.; Laaksonen, A. *J. Phys. Chem. B.* **2001**, *105*, 9308−9315.

(33) Paloncyova, M.; Berka, K.; Otyepka, M. *J. Chem. Theory Comput.* **2012**, *8*, 1200−1211.

(34) Rosso, L.; Gould, I. R. *J. Comput. Chem.* **2008**, *29*, 24−37.

(35) Wang, J.; Wolf, R. M.; Caldwell, J. W.; Kollman, P. A.; Case, D. A. *J. Comput. Chem.* **2004**, *25*, 1157−1174.

(36) Popplewell, J. F.; Swann, M. J.; Freeman, N. J.; McDonnell, C.; Ford, R. C. *Biochim. Biophys. Acta (BBA), Biomembr.* **2007**, *1768*, 13−20.

(37) Case, D. A.; Cheatham, T. E., III; Darden, T.; Gohlke, H.; Luo, R.; Merz, K. M., Jr.; Onufriev, A.; Simmerling, C.; Wang, B.; Woods, R. J. *J. Comput. Chem.* **2005**, *26*, 1668−1688.

(38) Wang, J.; Cieplak, P.; Kollman, P. A. *J. Comput. Chem.* **2000**, *21*, 1049−1074.

(39) Frisch, M. J.; Trucks, G. W.; Schlegel, H. B.; Scuseria, G. E.; Robb, M. A.; Cheeseman, J. R.; Scalmani, G.; Barone, V.; Mennucci, B.; Petersson, G. A. et al. *Gaussian09*, Revision A.02; Gaussian Inc.: Wallingford, CT, 2009.

(40) Martínez, L.; Andrade, R.; Birgin, E. G.; Martínez, J. M. *J. Comput. Chem.* **2009**, *30*, 2157−2164.

(41) Jorgensen, W. L.; Chandrasekhar, J.; Madura, J. D.; Impey, R. W.; Klein, M. L. *J. Chem. Phys.* **1983**, *79*, 926−935.

(42) Grossfield, A. WHAM: The Weighted Histogram Analysis Method v. 2.0.6; http://membrane.urmc.rochester.edu/content/wham.

(43) Marrink, S.-J.; Berendsen, H. J. C. *J. Phys. Chem.* **1994**, *98*, 4155−4168.

(44) Kumar, S.; Rosenberg, J. M.; Bouzida, D.; Swendsen, R. H.; Kollman, P. A. *J. Comput. Chem.* **1992**, *13*, 1011−1021.

(45) Li, L.; Vorobyov, I.; Allen, T. W. *J. Phys. Chem. B* **2008**, *112*, 9574−9587.

(46) Dorairaj, S.; Allen, T. W. *Proc. Natl. Acad. Sci. U.S.A.* **2007**, *104*, 4943−4948.

(47) Neale, C.; Tieleman, D. P.; Pomes, R. *J. Chem. Theory Comput.* **2011**, *7*, 4175−4188.
(48) Vorobyov, I.; Li, L.; Allen, T. W. *J. Phys. Chem. B* **2008**, *112*, 9588−9602.